

A flexible triboelectric tactile sensor for simultaneous material and texture recognition



Ziwu Song^{a,1}, Jihong Yin^{a,1}, Zihan Wang^{a,1}, Chengyue Lu^a, Ze Yang^{b,c}, Zihao Zhao^a, Zenan Lin^a, Jiyu Wang^{a,*}, Changsheng Wu^d, Jia Cheng^b, Yuan Dai^e, Yunlong Zi^f, Shao-Lun Huang^a, Xinlei Chen^a, Jian Song^g, Gang Li^g, Wenbo Ding^{a,h,**}

^a Tsinghua-Berkeley Shenzhen Institute, Tsinghua Shenzhen International Graduate School, Tsinghua University, 518055, China

^b State Key Laboratory of Tribology, Department of Mechanical Engineering, Tsinghua University, Beijing 100084, China

^c School of Engineering and Technology, China University of Geosciences (Beijing), Beijing 100083, China

^d Department of Mechanical Engineering, Center for Bio-Integrated Electronics, Northwestern University, Evanston, IL 60208, USA

^e Tencent Robotics X Lab, Shenzhen

^f Department of Mechanical and Automation Engineering and Shun Hing Institute of Advanced Engineering, The Chinese University of Hong Kong, New Territories, Hong Kong, China

^g Department of Electronic Engineering, Tsinghua University, Beijing 100084, China

^h RISC-V International Open Source Laboratory, Shenzhen 518055, China

ARTICLE INFO

Keywords:

Tactile sensing

Material/texture recognition

Signal decoupling

Triboelectric sensor

ABSTRACT

Electronic skin with tactile perception enables intelligent robots and prostheses to perform dexterous manipulation and natural interaction with the human and surroundings. However, using single tactile sensing mechanism to simultaneously percept geometry features and materials properties remains a challenge due to the bottleneck of signal decoupling. Herein, we report the MTsensing system – a wireless and fully-integrated tactile sensing system that can simultaneously recognize materials and textures based on a single flexible triboelectric sensor. The proposed triboelectric sensor converts touch into electrical signals and meanwhile, the signal processing pipeline decouples the signals into macro/micro features and feeds them into the corresponding deep learning models, which simultaneously predict the materials and textures of the contacted objects with the accuracies of 99.07% and 99.32%, respectively. The systematic integration of MTsensing hopes to pave the way for deploying low-cost and scalable electronic skin with multi-functional perceptions.

1. Introduction

The tactile sensation from electronic skin (e-skin) empowers the intelligent robotic system and prostheses for accurate motion trajectory planning [1], dexterous manipulation [2], safe operation [3], and diversified environment perception [4]. As an essential component towards intelligent sensing and control, tactile sensing leverage multiple mechanisms that have been developed to facilitate the tactile sensation of the robotic system [5], including piezoresistive array [6], soft optical strain sensor [7], magnetic microelectromechanical sensor (m-MEMS) [8], capacitive array [9], and piezoelectric sensor [10,11]. However, such single-mode sensors only percept mechanical stimuli, lacking

capability of sensing material properties. To this end, multimodal tactile sensors, which integrated more than one sensing mechanisms, enabled capturing both material properties and mechanical stimuli to facilitate robots with more accurate perception and interaction with surroundings [12,13]. Nevertheless, vertical stacking or planar arranging multiple sensors will unavoidably increase the thickness or reduce the spatial resolution. Moreover, signals simultaneously output from multiple sensors may mutual interfere with each other [14]; and the cost-effect issue is also hindering the popularization of commercial multimodal tactile sensor [15].

As a capacitive-like sensor [16–18], the emerging triboelectric nanogenerator (TENG) based sensors have shown the great potential in

* Corresponding author.

** Corresponding author at: Tsinghua-Berkeley Shenzhen Institute, Tsinghua Shenzhen International Graduate School, Tsinghua University, 518055, China.

E-mail addresses: jiyuwang@sz.tsinghua.edu.cn (J. Wang), ding.wenbo@sz.tsinghua.edu.cn (W. Ding).

¹ These authors contributed equally to this work.

realizing tactile sensing and e-skin, due to its low-cost, flexibility and wide choice of materials [19–25]. Although the advancement of TENG-based e-skin systems is improving the diversity [26–31] and usability of information [32–34], the data analysis pipelines of the existing systems [35–38] did not effectively decouple the material and texture features from the output signal of TENG, let alone to minimize the computational overhead of data analysis. Therefore, developing a system that can extract more hidden information in TENG signals while compatible with portable and wearable low-power embedded devices is expected to bring TENG-based e-skin systems to more broad applications.

Inspired by the perceptual habit of the human's fingertip [39,40] and motivated by the lack of signal decoupling, high fabrication cost, and devoid of system-level integration of existing tactile technologies [41], we developed a novel e-skin tactile sensor based on TENG, which only leveraged a single type of mechanism to realize multimodal sensing. Thanks to the inherent contact electrification properties and the adopted grating structure, the output signal's macro features (amplitude, trend, envelope, etc.) can be exploited for material recognition. In contrast, the micro features (frequency, changing point, variance, etc.) can be used for surface texture recognition. Considering the real application requirements, a signal decoupling method is proposed by introducing the wavelet transform. Based on this, a wireless and fully integrated system, "MTSensing", is implemented for real-time and simultaneous material and texture recognition. The MTSensing system contains three main parts, i.e., the fingertip sensor, the sensor-end circuit, and the display terminal. The sensor-end circuit encapsulated in a wearable bracelet is responsible for analysing the signal and wirelessly transmitting the result to the remote terminal for display. With the assistance of deep learning algorithms, we achieved high accuracies in the individual material (8 types, 98.45%) and texture (13 types, 98.03%) recognition tasks, and in the simultaneous material (4 types, 99.07%), texture (4

types, 99.32%) and object (16 combinational types, 98.40%) recognition tasks, respectively. Moreover, the fabrication of the sensing device and the rest hardware components system is fully compatible with the mature flexible printed circuit board (FPCB) processes, indicating the feasibility for low-cost and scalable deployment.

2. Results

2.1. MTSensing system for real-time and simultaneous material and texture recognition

As illustrated in Fig. 1a, the proposed MTSensing system provides simultaneous material and texture recognition for robotics and assistive technologies. The grating-structural free-standing TENG (GF-TENG) sensor attached to the fingertip of a robotic hand works as the front end, which generates analog sensing signals upon contact with objects. The signals are acquired and processed by the on-bracelet sensor-end circuit, where the features like the amplitude, frequency, local peak, and small vibration corresponding to different material and texture characteristics will be decoupled and further extracted to realize the simultaneous recognition. Finally, the waveforms and recognition results will be sent wirelessly to the remote terminal for real-time display.

The flexible GF-TENG sensor shown in Fig. 1b has a size of 20 mm by 15 mm with an overall thickness of 160 μm . The polyimide (PI) substrate attached to the robotic hand is robust to mechanical wearing and resilient to high-temperature soldering. The middle layer contains 20 μm thick interdigitated copper electrodes, where a 0.025 μm gold layer is deposited for antioxidant and long-standing. The top layer for triboelectrification with contact surfaces adopts the 3 M Kapton tape of 30 μm thickness. Details of a manufactured GF-TENG sensor can be found in Fig. S1. The output signals of the GF-TENG sensor are affected by the object materials, while the grating-structure design enables the

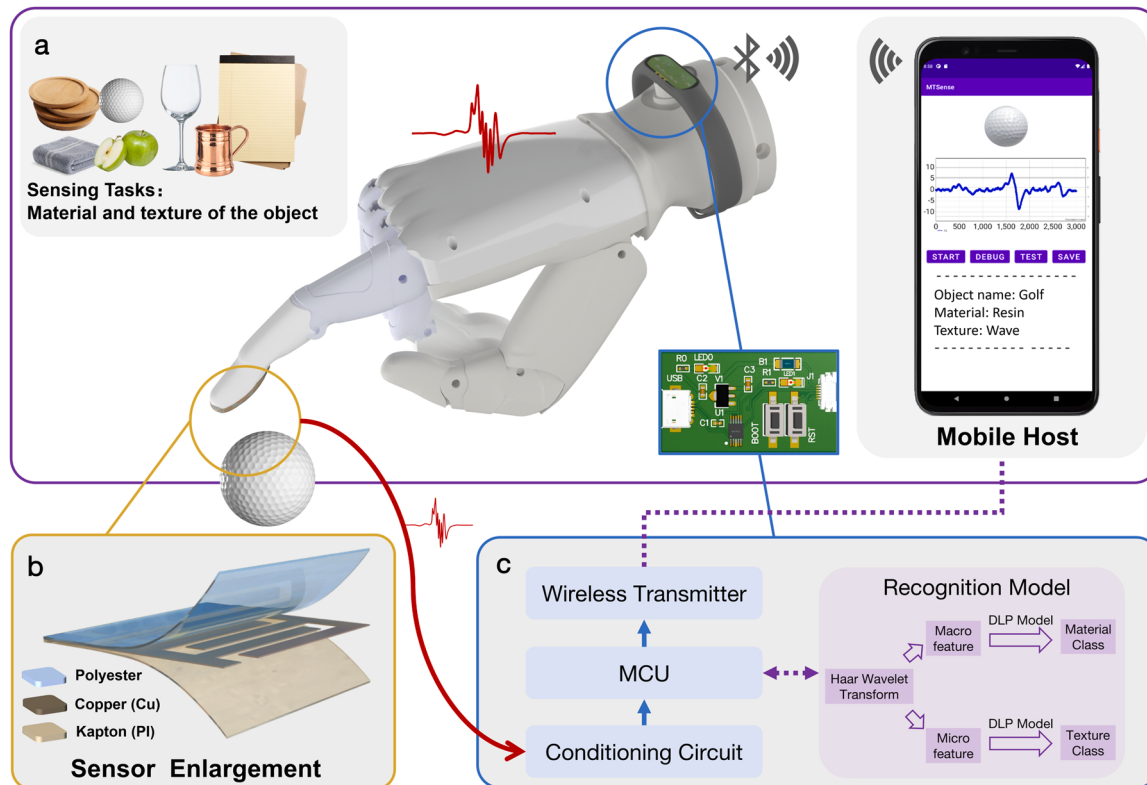


Fig. 1. Schematic illustration of the MTSensing system. (a) The schematic workflow of the MTSensing system: the flexible triboelectric sensor on fingertip converts the object features including material and texture characteristics into the signal and passes it to the customized PCB module for data processing and recognition, and the results will be wirelessly transmitted to and displayed on the mobile devices. (b) Layered illustration of the proposed fingertip grating-structural freestanding TENG (GF-TENG) sensor. (c) The system-level block diagram of the data acquisition and recognition processing on the PCB module.

sensor to be sensitive to the surface textures. Thanks to the mature FPCB process, the GF-TENG sensor is suitable for mass production.

The wearable bracelet (Fig. 1a) consists of three functional components: a signal conditioning circuit, a microcontroller unit (MCU) where the recognition model is applied, and a wireless transmitter (Fig. 1c). The conditioning circuit amplifies and filters the analog signals from the sensor and then converts the conditioned into digital form. Once the MCU receives the digital signals, the customized signal processing and deep learning-based recognition model distinguish the material and texture characteristics of the target objects. Finally, customized software on the smart device presents the recognition results and the real-time signals.

2.2. The optimization and characterization of the GF-TENG sensor

The electric output of TENG relies on the coupling effect of contact electrification and electrostatic induction. Specifically, the proposed GF-TENG sensor is based on the freestanding-mode TENG [42,43] and its working mechanism is shown in Fig. S2. To verify the working mechanism and theoretical output of the GF-TENG sensor, the finite element method (FEM) calculation under the open-circuit condition is carried out utilizing the COMSOL Multiphysics®. The electric potential

distributions of the GF-TENG sensor and the target object during four working stages can be found in Fig. S3. Further simulation studies by setting the material parameters of corresponding sensing objects indicate that the capacitance-like GF-TENG sensor can distinguish materials it slides over (Fig. S4). The FEM analysis [44] of the sensor sliding over various textures is shown in Fig. S5.

The interdigitated electrodes in GF-TENG can enhance the texture recognition capabilities. Nine GF-TENG sensors (Fig. S6) of different electrode size and gaps are fabricated (Fig. 2a) and tested under the same condition, horizontally sliding over the same standard texture with 8 N applied normal force (the chosen progress of the applied normal force is explained in Note S1). The generated time-domain signals of the nine sensors and the corresponding signal-to-noise ratio (SNR) are shown in Fig. 2b and c, respectively. The detailed calculation process of the SNR is provided in Note S2. The GF-TENG sensor with 2 mm electrode width and 2 mm electrode distance with the highest SNR is adopted throughout this project to extract the hidden features and restrain the noise.

The output performance of the sensor is characterized following the standard process [45]. The open-circuit voltage denoted as V_{oc} , the short circuit current denoted as I_{sc} and the transferred charge denoted as Q are measured, as shown in Fig. 2d-f, with a fixed sliding distance of 25 mm

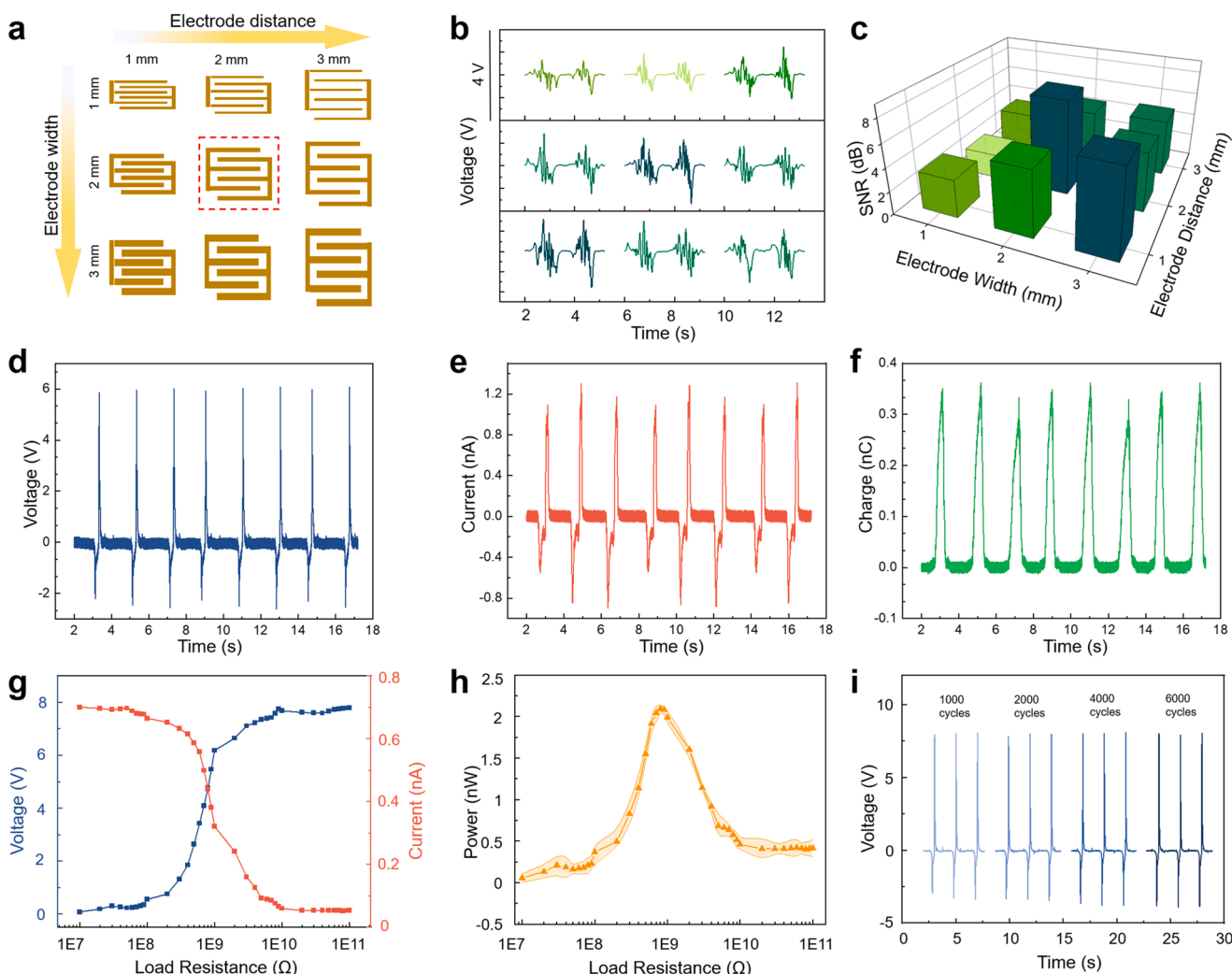


Fig. 2. Optimization and characterization of the proposed GF-TENG sensor. (a) The width of electrodes and distance between electrodes are adjusted from 1 mm to 3 mm. (b) The sensing waveforms of sliding on cotton fabric corresponding to the structures in (a). (c) The corresponding signal-to-noise ratio (SNR) is displayed in a 3-dimensional coordinate frame, which shows the maximum SNR is achieved when both the electrode width and distance are 2 mm. (d) The open-circuit voltage of the GF-TENG sensor. (e) Short-circuit current of the GF-TENG sensor. (f) Short-circuit charge transfer of the GF-TENG sensor. (g) Variation of the output voltage and current with the external load resistances. (h) The output power under different external load resistances. (i) Durability test of the GF-TENG sensor.

and a fixed sensing object of cotton covered on a smooth plane. The output performance of GF-TENG is investigated with external load resistance ranging from $100\text{ M}\Omega$ to $100\text{ G}\Omega$. As shown in Fig. 2g, the maximum power occurs by connecting $1\text{ G}\Omega$ load resistor (Fig. 2h). Therefore, $1\text{ G}\Omega$ is set as the optimal matching resistance in the following experiment. In addition, the durability test of the sensor is performed by sliding the GF-TENG sensor on cotton fabric attached to an

acrylic base for 6000 cycles, each cycle contains 20 mm forward and backward horizontal slides with the applied normal force of 8 N. The output voltage waveform shown in Fig. 2i reveals that there are no distinctive decreases or distortions during the durability test.

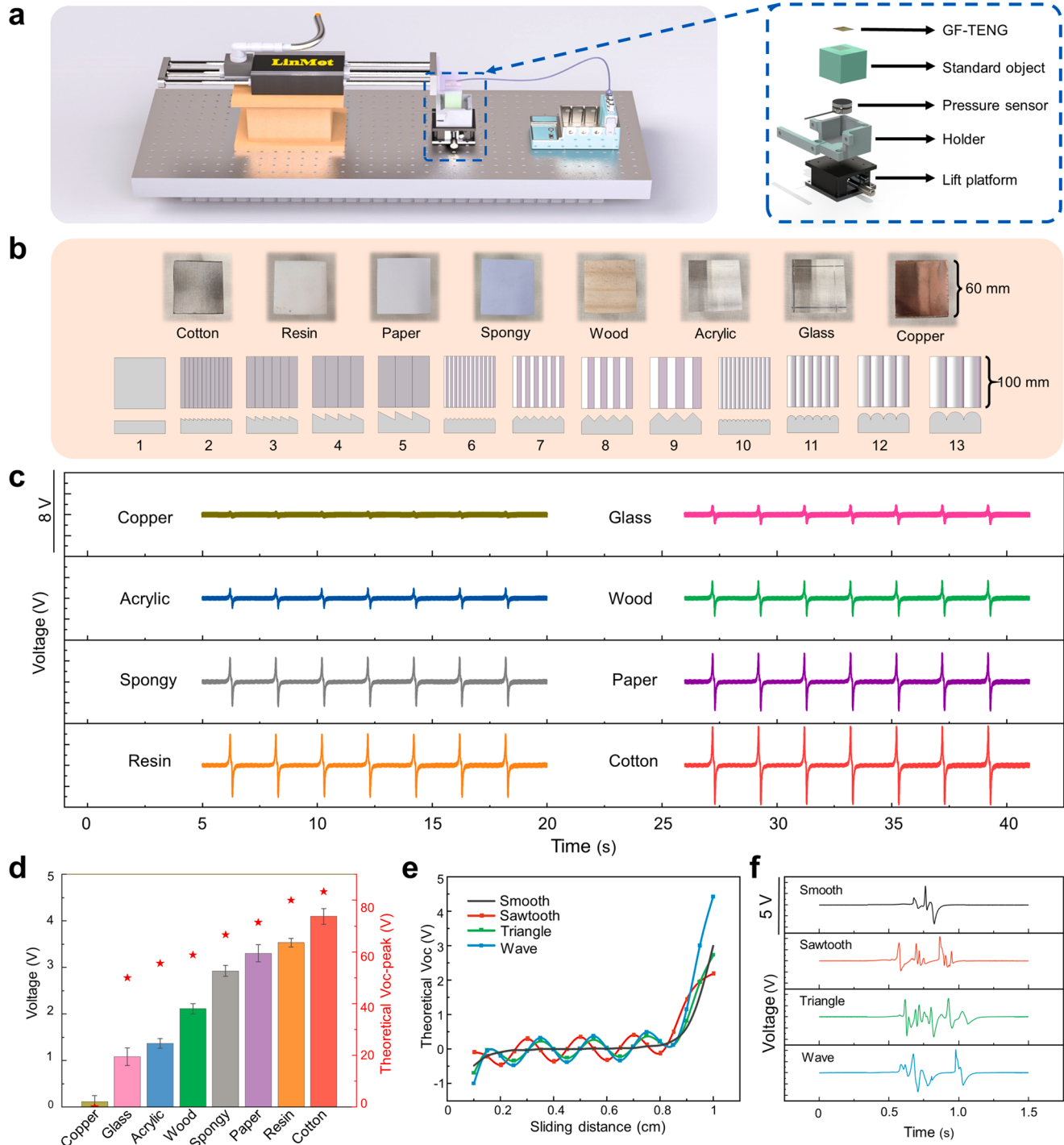


Fig. 3. Data collection of different materials and textures on a standardized platform. (a) The experimental platform for standardized testing and data collection. (b) The eight objects made of cotton, resin, paper, spongy, wood, acrylic, glass, copper, and 13 different textures designed based on flat, sawtooth, triangle and arch. The No. 1 texture is flat, the No. 2-No.5 textures are of sawtooth but with different densities, while the No. 6-No. 9 and No. 10-No.13 are of triangle and arch separately. (c) The measured voltage output of GF-TENG sensor sliding over eight materials. (d) Average peak voltage of GF-TENG sensor sliding over eight materials from measurement and simulation (red star), which is consist in trends. (e) The simulation result of sliding over four textures. (f) The measured signal of GF-TENG sensor sliding over four textures.

2.3. Capability characterization of the individual material and texture recognition tasks

An experimental platform is designed to investigate the influences of contact materials and textures on the sensing signal, where the sensor is characterized using standard objects. In the platform, the GF-TENG sensor is attached to a linear motor and slides on the standard objects with the reciprocating motion of the motor. Apart from the material types, the normal pressure applied on GF-TENG sensor can also influence the output signal during the reciprocating motion. A pressure sensor is mounted below the object, and a high precision lifting platform is used to offset the installation error to keep the normal pressure uniform, shown in the explosive view (Fig. 3a). At the beginning of each experiment, the high precision lifting platform is fine-tuned to adjust the pre-tightening pressure force to 8 N. To explore the influence of material and texture on GF-TENG sensor respectively, eight flat objects with different materials, and 13 resin made objects with different textures are designed (Fig. 3b).

Based on the dielectric properties of the materials, the simulations are conducted to investigate the influence of the materials on the free-standing TENG. Then the influence of electrodes on the output signal is further explored. Within the same sliding distance and different materials, the free-standing TENG generates signals with different maximum voltage. According to the comprehensive studies of free-standing TENG working principles [46], it can be concluded that the electron-capture ability of contact materials is a significant contributing factor that affects the amplitude of the output voltage. Fig. 3c shows the signals peak values from eight sensing targets with different materials varies. Therefore, this difference can be treated as the basis for differentiating different materials. The comparison average experimental voltage peak values (columns with different colors) and the theoretical voltage peak values (red star marks) of the eight materials is shown in Fig. 3d. The match of the trend of the average experimental peak voltages and the trend of the theoretical ones provides a strong reference for finding a stable and effective algorithm for material recognition [47].

To explore the influence of textures on sensing signals of the GF-TENG, the FEM simulation on the four resin samples of four surface textures, i.e., smooth, sawtooth, triangle and wavy surfaces, of which the corresponding results are depicted in Fig. 3e. The geometric characteristics of the signals are affected by the shape and density of textures, which can be used for texture recognition. As shown in Fig. 3f, signal waveforms from 4 textures are different. These characteristics show the possibility of the GF-TENG sensor to sense various textures. Therefore, if equipped with a proper feature extracting and classification algorithm, the GF-TENG sensor can be used for material and texture sensing by simply sliding over the sensing objects. To deploy deep-learning-based recognition model on MCU, a lighter network, one-dimensional CNN (1D CNN) is adopted to achieve recognition of materials and textures, respectively. Besides, 1D CNN has the specialty for extracting features from fixed-length time series segments, where the location of the features within the segment does not affect the classification result. To predetermine the scale of 1D CNN, a classical 1D CNN shown in Fig. S7a is designed to process the filtered signal directly, trained with the data from 8 materials and 13 textures separately. Note S3 shows the principle of training the model. The performance of the classical 1D CNN is presented in Fig. S7b–e.

2.4. Signal decoupling and capabilities of simultaneous material and texture recognition tasks

One important fact of the original signal is that the material information and texture information are coupled together. Fig. 3c reveals that material type affects the amplitude of the signal, which mainly contains the low-frequency but high-power components. Fig. 3f shows that standard textures made of the same material lead to the approximate upper bound but causes different quantities, positions and

durations of the peaks. The decoupling progress that separates the material and texture features from signals is critical for simultaneously distinguishes the material and texture of the sensing object. Here, wavelet decomposition is adopted for decoupling. During the wavelet decomposition, Haar wavelet bases are applied to represent the macro and micro features on two inner product spaces \mathbf{V} and \mathbf{W} separately, which are mutually orthogonal. Note S4 introduces the details in the calculation of the wavelet decomposition. The projection of the original signal on space \mathbf{V} with low resolution is used to represent the macro feature, while the projection on space \mathbf{W} with higher resolution but excluding amplitude information is used to reflect the micro feature. It should be noted that since both the material and applied force influence the signal amplitude, the accurate material classification of GF-TENG can only be made under controlled applied force. Nevertheless, we investigate the relationship between the pressure force and output signals of the GF-TENG sensor as shown in Fig. S8, where the applied pressure only affects the signal amplitude without changing the waveform modality. Further studies (Fig. S9) indicate that the GF-TENG can work as a pressure sensor with linearly response to the applied force.

Therefore, a new model that decouples macro and micro features and achieves simultaneous recognition is proposed based on Haar wavelet decomposition and 1D CNN to further improve the interpretability and obtain information on the two multimodalities, materials and textures. As illustrated in Fig. 4a, the recognition model contains two paralleled 1D CNNs, each consists of three convolutional layers and a fully connected layer which also serves as the classifier. The macro and micro features of the same scale are extracted by the Haar wavelet decomposition. The 1D CNN model fed with the macro features provides the material recognition result, while the 1D CNN model fed with micro features gives the texture recognition result. Finally, the material and texture recognition results are merged as the recognition result by combining the results of these two parallel 1D CNNs.

A dataset supporting the training on the proposed model is built, which contains 5600 sets of sensing signals of all possible combinations of four materials (copper, cotton, resin, and paper) and four textures (T1, T5, T9, T13, the numerical labels of the textures refer to Fig. 3b) accordingly (Fig. 4b). The decoupled features of selected samples of the sensing signals of 16 standard objects are shown in Fig. 4c (total comparisons between the original signals and the wavelet decomposition results are depicted in Fig. S10). The recognition results of the material recognition model and the texture recognition model are shown in Fig. 4d and Fig. 4e respectively. The simultaneous recognition results are the combinational effects of the material and texture recognition models. Here, the confusion matrix shown in Fig. 4f is calculated by the Kronecker product [48] (details in Note. S5) of the matrices in Fig. 4d and e, and the average recognition accuracies reach 99.07% and 99.32% separately. The dual recognition model performs better in the material recognition task and texture recognition task, compared to the recognition model without distinguishing macro and micro features. The variations of recognition accuracies come from the mutual effects of different pairs of materials and textures. The lowest recognition accuracy of all classes based on the combined dataset of materials and textures is 97.15% which appears on the T1 texture made of cotton. The highest recognition accuracy of 99.50% is acquired on the T13 texture made of resin. Besides, recognition on the 8 materials and 13 textures proposed in Fig. 3b is conducted, and the performances are shown in Figs. S11 and S12.

2.5. Design and demonstrations of the MTsensing system in real applications

To further explore the potential and the application of the proposed GF-TENG and simultaneous recognition model, a wearable MTsensing system is conceptualized for real-time data acquisition and recognition. The workflow of the MTsensing system is depicted in Fig. 5a. To match the high impedance of GF-TENG and convert current signals to the

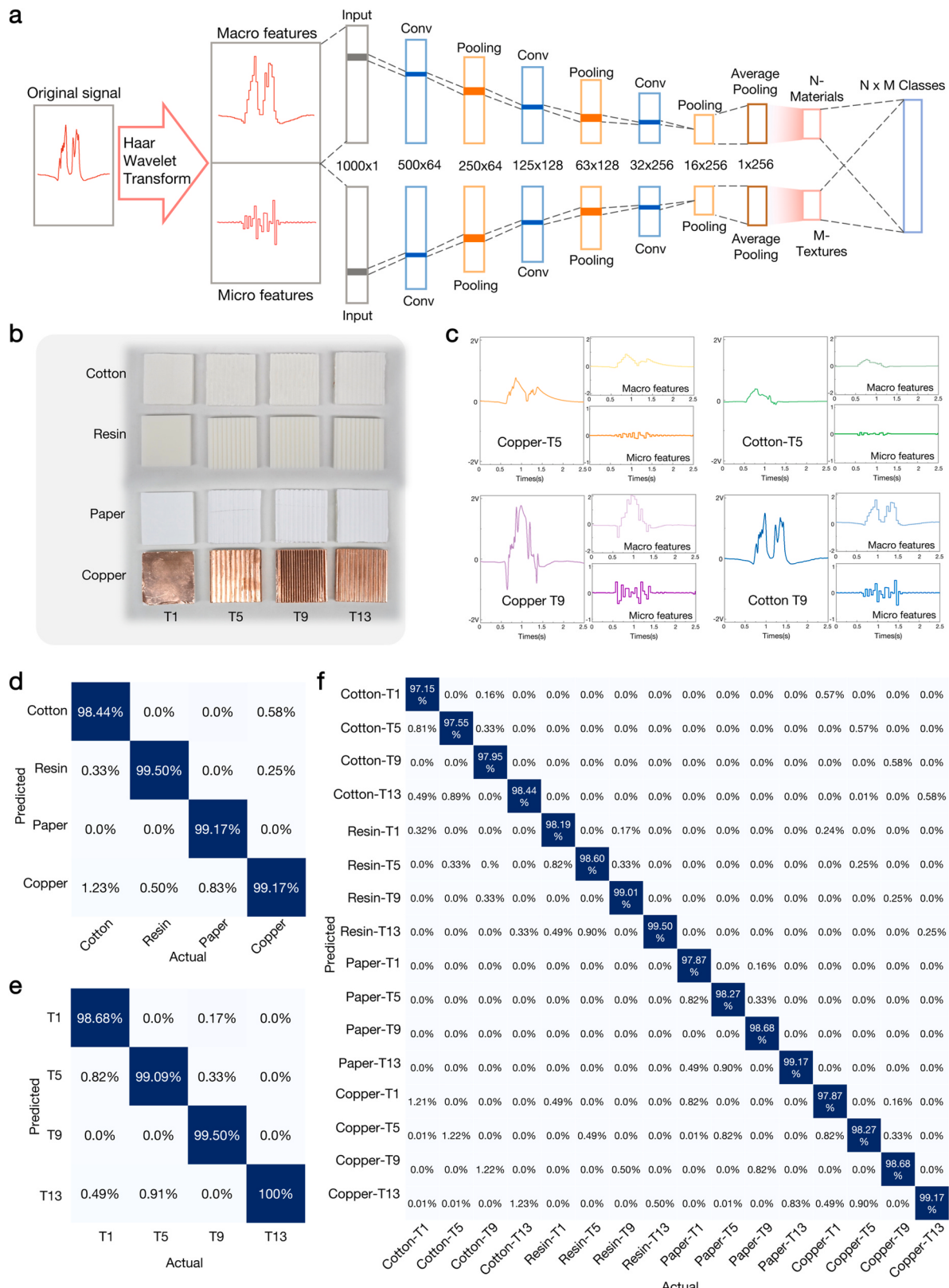


Fig. 4. Signal decoupling and simultaneous recognition model. (a) The architecture of the decoupling and customized 1D-CNN-based recognition model built to extract and classify features. (b) The 16 standard objects from the cross-pairing of 4 materials (copper, cotton, resin, and paper) and 4 textures (T1, T5, T9, T13, numerical labels refer to Fig. 3b) for simultaneous processing. (c) Selected samples of the sensing signals and the corresponding decoupled features. (d) The confusion matrix of the material recognition task on the 4 materials. (e) The confusion matrix of the texture recognition task on the 4 textures. (f) The confusion matrix of the merged recognition result on the 16 standard objects in (b).

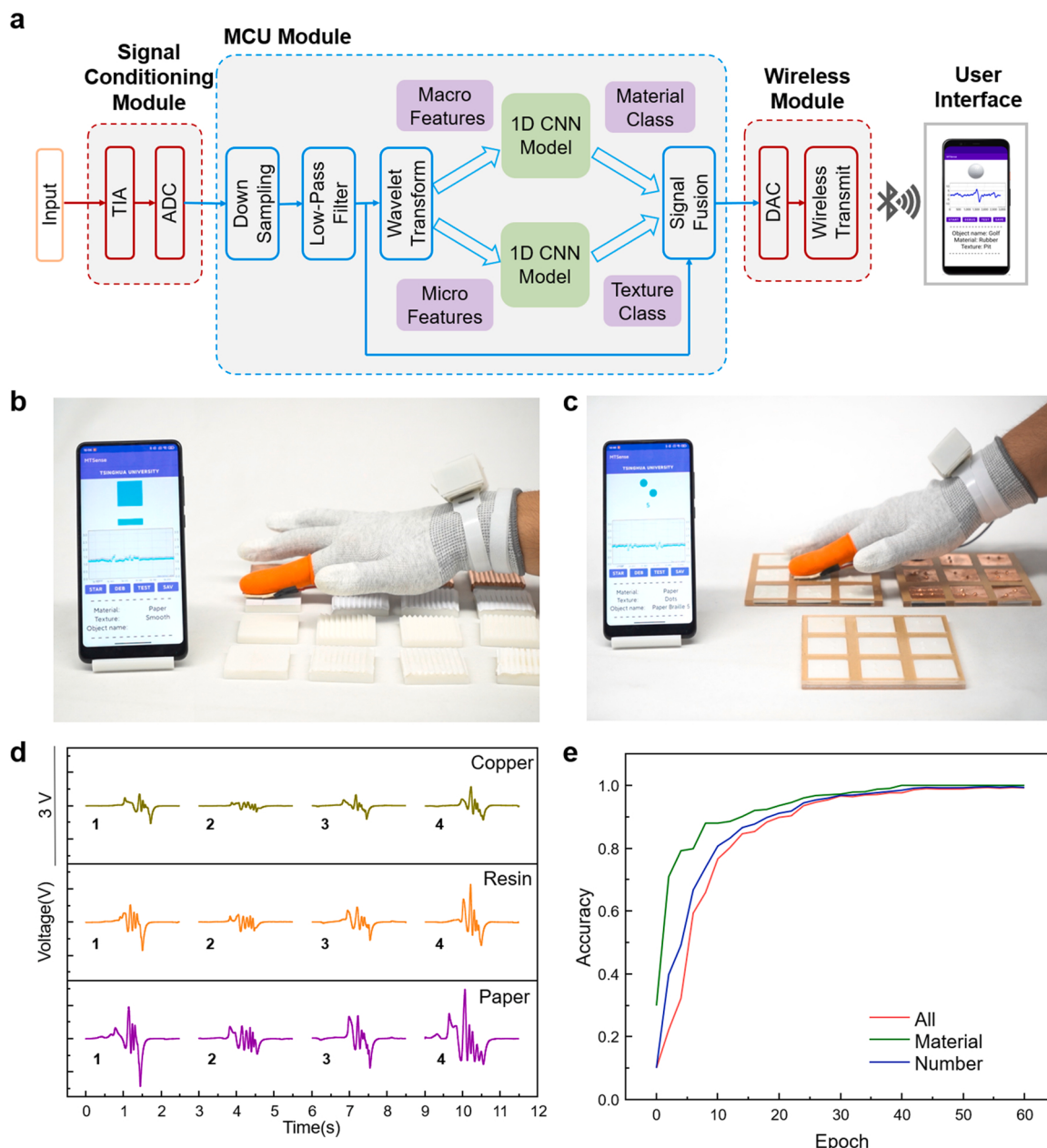


Fig. 5. Design and applications of MTSensing system. (a) The classical signal processing and deep learning algorithm assist the data process workflow of the MTSensing system. (b) Real time simultaneous material and texture recognition based on MTSeneing system. (c) Real time braille recognition based on MTSeneing system. (d) Sample of sensing signals of braille number made of 3 materials. (e) Training progress of the braille number recognition model.

acceptable voltage signals (0–3.3 V) of the analog to digital converter (ADC), a trans-impedance amplifier is deployed. Inside of the MCU, the converted digital signal is further down-sampled and goes through a low-pass filter. Then, the macro and micro features are extracted by Haar wavelet transform and fed into two independent deep learning models to support the material and texture recognition separately. At the end, both network outputs are combined to obtain the result. At this point, the recognition results will be sent to the display terminal via Bluetooth. To demonstrate the feasibility of this, the wearable MTSensing system is deployed on an actual human hand shown in Fig. 5b. The GF-TENG sensor is attached to the fingertip during sliding over the sensing targets. It achieves real-time simultaneously recognition of material and texture information of the 16 sensing targets introduced in Fig. 4b (see the Movie. S1). Based on these functions, more complicated and practical sensing applications can be developed.

Supplementary material related to this article can be found online at

[doi:10.1016/j.nanoen.2021.106798](https://doi.org/10.1016/j.nanoen.2021.106798).

Braille using special raised dots to provide visually impaired people with classifiable tactile perception needs long-term systematic learning. The dots of different braille words constitute special textures, and braille words on different household applications are of different materials. In Fig. 5c, a human hand with a GF-TENG sensor attached to the fingertip of the index finger randomly slides on the braille words including numbers one to nine made of resin, paper, and copper separately (the placement is shown in Fig. S13). Meanwhile, a smartphone displays the real-time waveform and the braille recognition result (see the Movie. S2). The classification model utilized in the on-bracelet circuit is pre-trained offline using the data of the sensing signals generated by the GF-TENG sensor. Fig. 5d shows the selected samples of the sensing signals corresponding to the braille boards made of copper, resin, and paper. The signals of numbers made of the same material show close amplitude but different waveforms, while the same numbers made of

different materials have similar waveforms but different amplitudes. The training progress on both material and braille recognition for the pre-training process is shown in Fig. 5e, where the joint recognition accuracy of 95.25% is reached within 60 iterations. Compared to traditional assistive braille recognition techniques, our MTsensing system can not only recognize the braille information but also distinguish the materials of the braille, which can be helpful on many occasions to help blind people and tactually impaired people better understand the braille on various infrastructures. Hence, the MTsensing system shows the potential for creating a promising assistive technology to allow visually or tactually impaired people better interact with modern smart devices and the environment around them.

Supplementary material related to this article can be found online at doi:10.1016/j.nanoen.2021.106798.

3. Discussion

We present a wireless and fully integrated tactile sensing system – MTsensing for real-time and simultaneous material and texture recognition. The design of the GF-TENG sensor is optimized by FEM to accurately reflect the texture features and contact materials. Then, signal processing pipeline made of wavelet decomposition-based signal decoupling followed by two paralleled 1D CNNs achieves material and texture recognition with over 98% accuracy. Finally, to demonstrate the reconfigurable usage of the MTsensing system, a braille recognition task is conducted to illustrate its application in assistive technology.

The attractive features of the MTsensing system include scalable fabrication processes and fully integrated material and texture sensing capability. The adoption of the mature FPCB process readily to large-scale produce the flexible sensors with arbitrary geometry. Therefore, the GF-TENG can be easily manufactured on a large scale and is adaptive to individualized applications. The sensing capability of textures and materials is established by innovatively decoupling a single signal stream. The proposed data processing model based on wavelet decomposition and 1D CNN is highly efficient, which can execute real-time analysis on embedded devices, such as low-power MCU with limited computing and memory resources.

In summary, the MTsensing system has great potential to empower robots with tactile sensation. To show this, a MTsensing system is deployed on a robot hand that achieves real-time recognition of common objects (see the Movie. S3, the tested objects are shown in Fig. S14). The proposed data processing model with low computational complexity enables the MTsensing system to independently work with low-cost edge devices. As a reconfigurable system, the application of MTsensing is not only limited to robotics. In the field of assistive technology, it is expected to restore the lost tactile sense of the impaired person with low response delay and high compatibility. Likewise, the reconfigurable design incorporates more modalities, such as shear stress, torsional stress, and temperature. Therefore, to expand its usage is worthy of exploring, a more complex deep learning network, processing data of more modalities, may designed and implemented in future works. Due to the limitations of the working mechanism of the GF-TENG, the simultaneous recognition of material and pressure have not been achieved. In future works, we expect to introduce new design to incorporate real-time pressure sensing and improve the conformability and stretchability of the device.

Supplementary material related to this article can be found online at doi:10.1016/j.nanoen.2021.106798.

4. Method

4.1. Fabrication of the grating-structure freestanding-TENG tactile sensor

The FPCB process is utilized to manufacture the soft substrate and the electrodes, where six strip electrodes are embedded in a 20 mm by 30 mm rectangular PI substrate. Each electrode is 20 mm in length and

2 mm in width, and the intervals of adjacent electrodes are 2 mm. The first, third, and fifth electrodes are connected to each other via holes and copper traces printed on the opposite side of the soft substrate. At the same time, the rest electrodes are also connected to each other in the same way symmetrically. Then, the Kapton tape, with the same size as the soft substrate and the thickness of 30 μm , is affixed on the electrodes side of the substrate. The fabrication price for each GF-TENG sensor is approximately 0.8 US dollars.

4.2. Design and fabrication of the wearable bracelet

The bracelet consists of a sensor-end circuit with three functional parts and a compact Li-ion battery for the power supply. The first functional part is a conditioning circuit that can amplify the small current signal and transform it into a voltage signal that matches the ADC; the second part is an MCU for signal processing and neural network inference; the last part is a wireless transmitter communicating with the remote terminal. Since the current signal generated by the sensor has a large output impedance, a low-power amplifier ADA4505 with high impedance and low bias current (0.5pA in typical) are selected for this design. Considering accuracy, sampling rate, multiple inputs and extensibility, we adopt AD7490, a 12-bit high speed, low power, 16-channel, successive approximation ADC to connect with the MCU via General Purpose Input/Output (GPIO) port. Considering the build-in with Bluetooth and Wi-Fi support and limited energy storage, ESP32-D2WD dual-core MCU with 2MB flash is selected for computational task and communication. The schematic circuit diagram is shown in Fig. S15.

4.3. FEM calculation details

FEM calculations are conducted to simulate the output performance of the GF-TENG. The composition and the applied structure parameters of the simulated GF-TENG sensor are identical to the real optimized GF-TENG (grating structure TENG with the electrode width of 2 mm and the electrode gap of 2 mm, consisting of a 0.018 mm copper electrode layer and a 0.065 mm Kapton frictional layer). The sensing progress is unified to a single direction sliding with 17 mm and 10 mm sliding distance for material and texture sensing progress, respectively. The thickness of the sensing object is 2 mm, and the material property of the sensing object is controlled by changing the permittivity. Furthermore, textures models are conducted with a uniform peak gap of 3 mm, and a peak thickness of 0.5 mm is built for the simulation of electric behavior on different texture types. The whole FEM calculation progress satisfies the law of conservation of electric charge, and the charge density distribution follows the working mechanism (Fig. S3).

4.4. Electric measurement and characterization

Field-emission scanning electron microscopy (Hitachi SU8010) is used to characterize the surface vias structure of the GF-TENG sensor (Fig. S16). A step motor (LinMot P01-37 \times 120-C/C1100) is used to provide standardized sliding progress. For the electric output measurements of the fingertip GF-TENG sensor, a programmable electrometer (Keithley Instruments 6514) is adopted to measure the voltages, currents and transferred charges. The NI 9223 and NI cDAQ 9174 modules are used to collect data. These methods are used for standardized data testing.

4.5. 1D CNN model architecture and training details

The 1D CNN model consists of a forward propagation path of three one-dimension convolutional layers, three pooling layers, and a fully connected layer which also serves as the classifier. Each convolutional layer is followed by a batch normalization layer and a ReLU (Rectified Linear Unit) activation layer. During training, 70% of the tactile sensing

dataset is used for training, rest for validation. The cross-entropy loss is utilized, and the whole model is trained using an adaptive moment estimation (Adam) optimizer with a learning rate of 0.0001 over 50 epochs. The batch size is adjusted to 128 to fit on the GPU. The program is developed using the Pytorch library, and the model is trained on a GeForce RTX 3090 GPU.

CRediT authorship contribution statement

W. Ding conceptualized and supervised the project. **W. Ding, Z. Song, J. Yin, Z. Wang, J. Wang, C. Lu, Z. Yang, Z. Zhao, Z. Lin, and J. Cheng** designed the experiment. **J. Yin and J. Wang** carried out the simulations. **Z. Song, C. Lu, and Z. Zhao** designed the software. **J. Yin, Z. Song, and Z. Wang** wrote the original draft. **Z.S., Z.W., J.Y., and Z.Y.** prepared the visualization. All authors discussed and reviewed the manuscript.

Declaration of Competing Interest

The authors declare that they have no known competing financial interests or personal relationships that could have appeared to influence the work reported in this paper.

Data and materials availability

All data are available in the main text or the [Supplementary Materials](#). The additional raw data or materials that support the findings of this study are available from the corresponding author upon reasonable request.

Acknowledgement

We acknowledge the assistance and advice of Mr. Junfei Chen and Ms. Xu Yang on the design of the PCB. We also thank Dr. Sixing Xu from Hunan University for the discussion on the TENG working mechanism. This work is supported in part by the National Natural Science Foundation of China under Grants 62104125 and 52007019, by Tsinghua-Foshan Innovation Special Fund (TFISF) 2020THFS0109, by the grant from the Institute for Guo Qiang of Tsinghua University 2020GQQ1004, by the Oversea Collaboration Funds of Tsinghua SIGS HW2021 and by the Scientific Research Start-up Funds of Tsinghua SIGS QD2021013C.

Appendix A. Supporting information

Supplementary data associated with this article can be found in the online version at [doi:10.1016/j.nanoen.2021.106798](https://doi.org/10.1016/j.nanoen.2021.106798).

References

- [1] Heidemann, G., Schopfer, M., Dynamic tactile sensing for object identification, in: : Proceedings of the IEEE Int. Conf. Robot. Autom., New Orleans, (2004), 813–818.
- [2] A. Yamaguchi, C.G. Atkeson, Recent progress in tactile sensing and sensors for robotic manipulation: can we turn tactile sensing into vision? *Adv. Robot.* 33 (2019) 661–673.
- [3] G. Pang, G. Yang, W. Heng, Z. Ye, X. Huang, H.Y. Yang, Z. Pang, CoboSkin: soft robot skin with variable stiffness for safer human–robot collaboration, *IEEE Trans. Ind. Electron.* 68 (2021) 3303–3314.
- [4] R.S. Dahiya, G. Metta, M. Valle, G. Sandini, Tactile sensing—from humans to humanoids, *IEEE Trans. Robot.* 26 (2010) 1–20.
- [5] Baishya, S., and Bauml, B., Robust Material Classification with a Tactile Skin Using Deep Learning. in: IEEE Int. Conf. Intell. Robot. Syst., Daejeon, (2016), pp. 8–15.
- [6] S. Sundaram, P. Kellnhofer, Y. Li, J.Y. Zhu, A. Torralba, W. Matusik, Learning the signatures of the human grasp using a scalable tactile glove, *Nature* 569 (2019) 698–702.
- [7] H. Zhao, J. Jalving, R. Huang, R. Knepper, A. Ruina, R. Shepherd, A helping hand: soft orthosis with integrated optical strain sensors and EMG control, *IEEE Robot. Autom. Mag.* 23 (2016) 55–64.
- [8] J. Ge, X. Wang, M. Drack, O. Volkov, M. Liang, G.S. Cañón Bermúdez, R. Illing, C. Wang, S. Zhou, J. Fassbender, M. Kaltenbrunner, D. Makarov, A bimodal soft electronic skin for tactile and touchless interaction in real time, *Nat. Commun.* 10 (2019) 4405.
- [9] C.M. Boutry, M. Negre, M. Jorda, O. Vardoulis, A. Chortos, O. Khatib, Z. Bao, A hierarchically patterned, bioinspired e-skin able to detect the direction of applied pressure for robotics, *Sci. Robot.* 3 (3 0) (2018) aa9694.
- [10] X. Wang, W.Z. Song, M.H. You, J. Zhang, M. Yu, Z. Fan, S. Ramakrishna, Y.Z. Long, Bionic single-electrode electronic skin unit based on piezoelectric nanogenerator, *ACS Nano* 12 (2018) 8588–8596.
- [11] W. Lin, B. Wang, G. Peng, Y. Shan, H. Hu, Z. Yang, Skin-inspired piezoelectric tactile sensor array with crosstalk-free row+column electrodes for spatiotemporally distinguishing diverse stimuli, *Adv. Sci.* 8 (2021), 2002817.
- [12] G. Li, S. Liu, L. Wang, R. Zhu, Skin-inspired quadruple tactile sensors integrated on a robot hand enable object recognition, *Sci. Robot.* 5 (2020) abc8134.
- [13] F. Sun, B. Fang, H. Xue, H. Liu, H. Huang, A novel multi-modal tactile sensor design using thermochromic material, *Sci. China Inf. Sci.* 62 (2019), 214201.
- [14] J.C. Yang, J. Mun, S.Y. Kwon, S. Park, Z. Bao, S. Park, Electronic skin: recent progress and future prospects for skin-attachable devices for health monitoring, robotics, and prosthetics, *Adv. Mater.* 31 (2019), e1904765.
- [15] Fishel, J.A., Loeb, G.E., Sensing tactile microvibrations with the BioTac — Comparison with human sensitivity. in: Proceedings of the IEEE Int. Conf. Biomed. Robot. Biomech., Rome, (2012) 1122–1127.
- [16] Alagi, H., et al., Material recognition using a capacitive proximity sensor with flexible spatial resolution. in: Proceedings of the IEEE Int. Conf. Intell. Robot. Syst., Madrid, (2018) 6284–6290.
- [17] C. Larson, J. Spjut, R. Knepper, R. Shepherd, A deformable interface for human touch recognition using stretchable carbon nanotube dielectric elastomer sensors and deep neural networks, *Soft Robot.* 6 (2019) 611–620.
- [18] Ding, Y., et al., Using Machine Learning for Material Detection with Capacitive Proximity Sensors. in: Proceedings of the IEEE Int. Conf. Intell. Robot. Syst., Las Vegas, (2020) 10424–10429.
- [19] Y. Song, J. Min, Y. Yu, H. Wang, Y. Yang, H. Zhang, W. Gao, Wireless battery-free wearable sweat sensor powered by human motion, *Sci. Adv.* 6 (2020) eaay9842.
- [20] X. Peng, K. Dong, C. Ye, Y. Jiang, S. Zhai, R. Cheng, D. Liu, X. Gao, J. Wang, Z. L. Wang, A breathable, biodegradable, antibacterial, and self-powered electronic skin based on all-nanofiber triboelectric nanogenerators, *Sci. Adv.* 6 (2020), eaba9624.
- [21] G. Yao, L. Xu, X. Cheng, Y. Li, X. Huang, W. Guo, S. Liu, Z.L. Wang, H. Wu, Bioinspired triboelectric nanogenerators as self-powered electronic skin for robotic tactile sensing, *Adv. Funct. Mater.* 30 (2019), 1907312.
- [22] Y. Jiang, K. Dong, X. Li, J. An, D. Wu, X. Peng, J. Yi, C. Ning, R. Cheng, P. Yu, Z. L. Wang, Stretchable, washable, and ultrathin triboelectric nanogenerators as skin-like highly sensitive self-powered haptic sensors, *Adv. Funct. Mater.* 31 (2020), 2005584.
- [23] Y.C. Lai, J. Deng, R. Liu, Y.C. Hsiao, S.L. Zhang, W. Peng, H.M. Wu, X. Wang, Z. L. Wang, Actively perceiving and responsive soft robots enabled by self-powered, highly extensible, and highly sensitive triboelectric proximity- and pressure-sensing skins, *Adv. Mater.* 30 (2018), 1801114.
- [24] Z. Ren, J. Nie, J. Shao, Q. Lai, L. Wang, J. Chen, X. Chen, Z.L. Wang, Fully elastic and metal-free tactile sensors for detecting both normal and tangential forces based on triboelectric nanogenerators, *Adv. Funct. Mater.* 28 (2018), 1802989.
- [25] X. Xie, Y. Chen, J. Jiang, J. Li, Y. Yang, Y. Liu, L. Yang, X. Tu, X. Sun, C. Zhao, M. Sun, Z. Wen, Self-powered gyroscope angle sensor based on resistive matching effect of triboelectric nanogenerator, *Adv. Mater. Technol.* 6 (2021), 2100797.
- [26] G. Lee, J.H. Son, S. Lee, S.W. Kim, D. Kim, N.N. Nguyen, S.G. Lee, K. Cho, Fingertip-inspired multimodal electronic skin for material discrimination and texture recognition, *Adv. Sci.* 8 (2021), 2002606.
- [27] Y. Wang, H. Wu, L. Xu, H. Zhang, Y. Yang, Z.L. Wang, Hierarchically patterned self-powered sensors for multifunctional tactile sensing, *Sci. Adv.* 6 (2020) eabb9083.
- [28] Y. Jiang, Y. Wang, Y.K. Mishra, R. Adelung, Y. Yang, Stretchable CNTs-ecoflex composite as variable-transmittance skin for ultrasensitive strain sensing, *Adv. Mater. Technol.* 3 (2018), 1800248.
- [29] Y.W. Cai, X.N. Zhang, G.G. Wang, G.Z. Li, D.Q. Zhao, N. Sun, F. Li, H.Y. Zhang, J. C. Han, Y. Yang, A flexible ultra-sensitive triboelectric tactile sensor of wrinkled PDMS/MXene composite films for E-skin, *Nano Energy* 81 (2021), 105663.
- [30] T. Zhang, Z. Wen, H. Lei, Z. Gao, Y. Chen, Y. Zhang, J. Liu, Y. Xie, X. Sun, Surface-microengineering for high-performance triboelectric tactile sensor via dynamically assembled ferrofluid template, *Nano Energy* 87 (2021), 106215.
- [31] H. Lei, Y. Chen, Z. Gao, Z. Wen, X. Sun, Advances in self-powered triboelectric pressure sensors, *J. Mater. Chem. A* 9 (2021) 20100–20130.
- [32] M. Ha, S. Lim, S. Cho, Y. Lee, S. Na, C. Baig, H. Ko, Skin-Inspired hierarchical polymer architectures with gradient stiffness for spacer-free, ultrathin, and highly sensitive triboelectric sensors, *ACS Nano* 12 (2018) 3964–3974.
- [33] S. Chun, C. Pang, S.B. Cho, A micropillar-assisted versatile strategy for highly sensitive and efficient triboelectric energy generation under in-plane stimuli, *Adv. Mater.* 32 (2020), 1905539.
- [34] X. Pu, M. Liu, X. Chen, J. Sun, C. Du, Y. Zhang, J. Zhai, W. Hu, Z.L. Wang, Ultrastretchable, transparent triboelectric nanogenerator as electronic skin for biomechanical energy harvesting and tactile sensing, *Sci. Adv.* 3 (2017), e1700015.
- [35] X. Zhao, Z. Zhang, L. Xu, F. Gao, B. Zhao, T. Ouyang, Z. Kang, Q. Liao, Y. Zhang, Fingerprint-inspired electronic skin based on triboelectric nanogenerator for fine texture recognition, *Nano Energy* 85 (2021), 106001.
- [36] T. Jin, Z. Sun, L. Li, Q. Zhang, M. Zhu, Z. Zhang, G. Yuan, T. Chen, Y. Tian, X. Hou, C. Lee, Triboelectric nanogenerator sensors for soft robotics aiming at digital twin applications, *Nat. Commun.* 11 (2020) 5381.
- [37] Z. Sun, M. Zhu, Z. Zhang, Z. Chen, Q. Shi, X. Shan, R.C.H. Yeow, C. Lee, Artificial intelligence of things (AIoT) enabled virtual shop applications using self-powered sensor enhanced soft robotic manipulator, *Adv. Sci.* 8 (2021), 2100230.

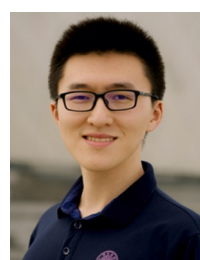
- [38] T. Zhang, L. Xie, J. Li, Z. Huang, H. Lei, Y. Liu, Z. Wen, Y. Xie, X. Sun, All-in-one self-powered human-machine interaction system for wireless remote telemetry and control of intelligent cars, *Nanomaterials* 11 (2021) 2711.
- [39] Y. Shao, V. Hayward, Y. Visell, Compression of dynamic tactile information in the human hand, *Sci. Adv.* 6 (2020), eaaz1158.
- [40] S. Chun, J.S. Kim, Y. Yoo, Y. Choi, S.J. Jung, D. Jang, G. Lee, K.I. Song, K.S. Nam, I. Youn, D. Son, C. Pang, Y. Jeong, H. Jung, Y.J. Kim, B.D. Choi, J. Kim, S.P. Kim, W. Park, S. Park, An artificial neural tactile sensing system, *Nat. Electron.* 4 (2021) 429–438.
- [41] B. Shih, D. Shah, J. Li, T.G. Thuruthel, Y.L. Park, F. Iida, Z. Bao, R. Kramer-Bottiglio, M.T. Tolley, Electronic skins and machine learning for intelligent soft robots, *Sci. Robot.* 5 (2020) aaz9239.
- [42] S. Niu, Y. Liu, X. Chen, S. Wang, Y.S. Zhou, L. Lin, Y. Xie, Z.L. Wang, Theory of freestanding triboelectric-layer-based nanogenerators, *Nano Energy* 12 (2015) 760–774.
- [43] S. Wang, Y. Xie, S. Niu, L. Lin, Z.L. Wang, Freestanding triboelectric-layer-based nanogenerators for harvesting energy from a moving object or human motion in contact and non-contact modes, *Adv. Mater.* 26 (2014) 2818–2824.
- [44] W. Yang, X. Wang, H. Li, J. Wu, Y. Hu, Z. Li, H. Liu, Fundamental research on the effective contact area of micro-/nano-textured surface in triboelectric nanogenerator, *Nano Energy* 57 (2019) 41–47.
- [45] W. Yang, J. Chen, G. Zhu, X. Wen, P. Bai, Y. Su, Y. Lin, Z. Wang, Harvesting vibration energy by a triple-cantilever based triboelectric nanogenerator, *Nano Res.* 6 (2013) 880–886.
- [46] S. Niu, Y. Liu, S. Wang, L. Lin, Y.S. Zhou, Y. Hu, Z.L. Wang, Theoretical investigation and structural optimization of single-electrode triboelectric nanogenerators, *Adv. Funct. Mater.* 24 (2014) 3332–3340.
- [47] R.D.I.G. Dharmasena, K.D.G.I. Jayawardena, C.A. Mills, J.H.B. Deane, J.V. Anguita, R.A. Dorey, S.R.P. Silva, Triboelectric nanogenerators: providing a fundamental framework, *Energy Environ. Sci.* 10 (2017) 1801–1811.
- [48] C.F. Van Loan, The ubiquitous Kronecker product, *J. Comput. Appl. Math.* 123 (2000) 85–100.



Ziwei Song is a Ph.D. student majoring in Data Science and Information Technology in Tsinghua-Berkeley Shenzhen Institute, Tsinghua University. He received his B.S. degree (Hons.) in Mechanical Engineering from Nanjing University of Science and Technology in 2020. His research interests mainly focus on tactile sensing and soft robotics.



Jihong Yin received the BEng. Degree from College of Science, Nanjing University of Aeronautics and Astronautics in 2019. He is currently a second-year master student majored in Data Science and Information Technology at Smart Sensing and Robotics (SSR) group, Tsinghua University. His research interests include soft robotics, robotic sensing and HMI.



Zihan Wang received the dual BEng. degrees (1st class Hons.) from School of Telecommunications Engineering, Xidian University and Edinburgh Centre for Robotics, Heriot-Watt University, respectively in 2019. He is currently pursuing his Ph.D. degree in Data Science and Information Technology at Smart Sensing and Robotics (SSR) group, Tsinghua University. His research interests include self-powered sensors, Internet of Things (IoTs), and robotics.



Chengyue Lu received the BS degree from School of Electrical and Information Engineering, Hunan University of Technology in 2020. He is now a research assistant in Data Science and Information Technology at Smart Sensing and Robotics (SSR) group, Tsinghua University. His research interests include machine learning, Vehicle to Everything (V2X), Internet of Things (IoTs), and robotics.



Ze Yang received his B.S. and M.S. degrees in mechanical engineering from Hubei University of Arts and Science and Beihua University in 2015 and 2018, respectively. He is currently pursuing the Ph.D. degree in mechanical engineering with the China University of Geosciences (Beijing) and Tsinghua University. His main research interests include triboelectric nanogenerator, energy harvesting and self-powered system.



Zihao Zhao received his B.S. degree in University of Electronic Science and Technology of China (UESTC) in 2021. He is currently pursuing his M.S. degree in Data Science and Information Technology at Smart Sensing and Robotics (SSR) group, Tsinghua University. His research interests include Internet of Things (IoTs), Federated Learning, and Machine Learning.



Zenan Lin received his B.S. degree in Electrical Engineering and Automation from China University of Mining and Technology in 2021. He is currently pursuing his M.S. degree in Data Science and Information Technology at Smart Sensing and Robotics (SSR) group, Tsinghua University. His research interests include Tactile sensing, Power management system of TENG.



Jiyu Wang received his B.S. and Ph.D. degree in Electrical Engineering from Chongqing University in 2013 and 2019, respectively. He is currently a Post-Doctoral Fellow in Tsinghua-Berkeley Shenzhen Institute (TBSI). He has authored over 20 journal and conference papers and received the National Scholarship and the Excellent Doctoral Dissertation of Chongqing Province in 2018 and 2020. His main research interests include energy harvesting, self-powered electronics, and additive manufacturing.



Changsheng Wu received the B.E. degree in Engineering Science from National University of Singapore in 2013 and the Ph.D. degree in Materials Science and Engineering from Georgia Institute of Technology in 2019. He is now a postdoctoral fellow at Querrey Simpson Institute for Bioelectronics, Northwestern University. His research interests include bioelectronics, energy harvesting, self-powered sensors, electromechanical systems, and advanced manufacturing.



Xinlei Chen received his BS and MS degrees from Tsinghua University in 2009 and 2012 respectively. He received his PhD degree from Carnegie Mellon University in 2018 and worked as a postdoctoral research fellow at Carnegie Mellon University from 2018 to 2020. He is now a tenure-track assistant professor and PhD supervisor at Tsinghua-Berkeley Shenzhen Institute, Tsinghua Shenzhen International Graduate School, Tsinghua University. His research interests include AIoT, smart sensing, cyber physical system, wearable devices, brain computer interface, mobile computing and etc.



Jia Cheng is an associate professor working in Department of Mechanical Engineering at Tsinghua University. He earned both his B.E. and Ph.D. at Tsinghua University in 2002 and 2008, respectively. His research spans areas including mechanical design, triboelectric nanogenerator, microplasma and discharge. He had managed a project of Important National Science & Technology Specific Projects (No.2) and won the Second-Class Prize of National Sci-Tech Advancement in 2009.



Jian Song received the B. Eng and Ph.D. degrees in electrical engineering from Tsinghua University, Beijing, China, in 1990 and 1995, respectively. Currently, he is the Professor at Electronic Engineering Department of Tsinghua University and the director of DTV Technology R&D Center. His current research interest is in the area of broadband wireless multimedia transmission technologies and networking. Dr. Song has published more than 300 peer-reviewed journal and conference papers. He holds two U.S. and more than 80 Chinese patents. He is Fellow of both IEEE and IET.



Yuan Dai received her B.S. degree from University of Illinois, Urbana-Champaign (UIUC) in 2012, and her Ph.D. degree from University of California, Los Angeles (UCLA) in 2018, both in electrical and computer engineering. Since Jan. 2019, she has been with Tencent, where she is a senior researcher with Robotics X. She has authored or coauthored more than 20 journal and conference papers and has been authorized 9 patents. Her main research interests include Nano/Microelectromechanical Systems (N/MEMS), sensors, actuators, wearable devices, VR, machine learning, Internet of Things, and robotics.



Gang Li received the B.S. and Ph.D. degrees in electronic engineering from Tsinghua University, Beijing, China, in 2002 and 2007, respectively. Since July 2007, he has been with the Faculty of Tsinghua University, where he is a Professor with the Department of Electronic Engineering. From 2012–2014, he visited The Ohio State University, Columbus, OH, USA, and Syracuse University, Syracuse, NY, USA. He has authored or coauthored more than 160 journal and conference papers. He is the Author of the book, Advanced Sparsity-Driven Models and Methods for Radar Applications. His research interests include radar signal processing, distributed signal processing, sparse signal processing, remote sensing, and information fusion.



Yunlong Zi is an Assistant Professor in Department of Mechanical and Automation Engineering at the Chinese University of Hong Kong since 2017. Dr. Zi received his Ph.D. in Physics from Purdue University in 2014; his Bachelor of Engineering in Materials Science and Engineering from Tsinghua University in 2009. Before joining CUHK, he worked as a Postdoctoral Fellow at Georgia Institute of Technology during 2014–2017. His current research interests mainly focus on high-efficiency mechanical energy harvesting through triboelectric nanogenerators (TENG), triboelectric effect, discharge, TENG triggered high-voltage applications, and self-powered systems.



Wenbo Ding received the BS and Ph.D. degrees (Hons.) from Tsinghua University in 2011 and 2016, respectively. He worked as a postdoctoral research fellow at Georgia Tech under the supervision of Professor Z. L. Wang from 2016 to 2019. He is now a tenure-track assistant professor and PhD supervisor at Tsinghua-Berkeley Shenzhen Institute, Tsinghua Shenzhen International Graduate School, Tsinghua University, where he leads the Smart Sensing and Robotics (SSR) group. His research interests are diverse and interdisciplinary, which include self-powered sensors, energy harvesting, and wearable devices for health and soft robotics with the help of signal processing, machine learning, and mobile computing. He has received



Shao-Lun Huang received the B.S. degree with honor in 2008 from the Department of Electronic Engineering, National Taiwan University, Taiwan, and the M.S. and Ph.D. degree in 2010 and 2013 from the Department of Electronic Engineering and Computer Sciences, Massachusetts Institute of Technology. From 2013–2016, he was working as a postdoctoral researcher jointly in the Department of Electrical Engineering at the National Taiwan University and the Department of Electrical Engineering and Computer Science at the Massachusetts Institute of Technology. Since 2016, he has joined Tsinghua-Berkeley Shenzhen Institute, where he is currently an associate professor. His research interests include information

theory, communication theory, machine learning, and social networks.